Physica Scripta. Vol. 41, 83–87, 1990.

Adsorbate-to-Si(100) Bonding Coordination Numbers and Structural Determinations from Synchrotron Photoemission Studies

D. H. Rich, A. Samsavar, T. Miller, and T. -C. Chiang

Department of Physics and Materials Research Laboratory, University of Illinois at Urbana-Champaign, 1110 West Green Street, Urbana, IL 61801, U.S.A.

Received July 16, 1989; accepted September 13, 1989

Abstract

The initial stages of interface formation between In, Sb, Sn, and Ag adsorbates and the Si(100)-(2 × 1) surface have been examined with high resolution core-level photoemission spectroscopy. In each case, the Si 2*p* surface-shifted core-level component is seen to be converted into a component which is indistinguishable from the bulk component through adsorption. The average number of Si surface dimer atoms modified in the presence of an adatom, which is referred to as the adsorbate-to-Si bonding coordination number (BCN), is obtained for various coverages. The relative homogeneity of the adsorbate site bonding is evaluated by examining the line shapes of the adsorbate core-level spectra. The In-to-Si BCN is 3 for very low coverages and decreases to 2 for 1/2-monolayer coverage. The results are consistent with an In/Si(100)-(2 × 2) structural model which involves sp^2 hybrid bonding of In dimers. The Sn 4*d* core levels reveal the existence of two different Sn bonding sites which form sp^3 and s^2p^2 hybrid bonding configurations; a structural model for the Sn/Si(100)-*c*(4 × 4) is presented. The Ag-to-Si BCN measurement indicates that adsorbed Ag forms linear *sp* hybrid bonds between two neighboring Si dimers along the direction of dimerization at low coverages. Sb chemisorption is found to yield a BCN behavior similar to that of In.

1. Introduction

In order to fully assess the potentiality for attaining and optimizing the epitaxial growth of high-quality thin films on clean semiconductor substrates, it is essential that the basic electronic, chemical, and structural properties during the initial stages of interface formation be well established. Despite the significant volume of experimental and theoretical research performed to ascertain the structural configurations of clean and adsorbate-covered surfaces, definitive atomic geometries are known confidently for only a handful of systems. The dimer nature of the Si(100)-(2 × 1) surface has been confirmed through scanning tunneling microscopy (STM) [1], and this rudimentary structure, possessing one dangling bond per surface atom, provides a convenient gauge for examining basic adsorption processes occurring at the atomic level. In this report, we examine the adsorption of In [2], Sb [3], Sn [4], and Ag [5], on the Si(100) surface using high-resolution core-level spectroscopy and high-energy electron diffraction (HEED). Surface atoms existing in inequivalent sites due to reconstruction and chemisorption often exhibit binding energy shifts which are measurable with photoemission. The average number of Si surface dimer atoms which are modified in the presence of an adsorbate atom, which we term the adsorbate-to-substrate bonding coordination number (BCN), is obtained by analyzing the Si 2*p* core-level line shape for various submonolayer adsorbate coverages. An examination of the adsorbate core levels is used to evaluate the variability in the adsorbate-site bonding. From the photoemission and HEED results, the number of possible atomic structures for the adsorbates are reduced and models are presented. Because of space limitations, some details are referred to previous reports [2–5].

2. Experiment

The photoemission experiments were carried out using synchrotron radiation from the University-of-Illinois beam line on the 1 GeV storage ring at the Synchrotron Radiation Center of the University of Wisconsin-Madison at Stoughton, Wisconsin. Light from the ring was dispersed by an extended-range grating monochromator [6]. An angle-integrating hemispherical analyzer was used for collecting and analyzing the photoelectrons. The bulk- and surface-sensitive Si 2*p* core-level spectra were taken with photon energies of 108 eV and 140–150 eV, respectively. The overall instrumental resolution was ~0.2 eV. The photoemission chamber also had the capabilities of HEED, Auger spectroscopy, and molecular beam epitaxy (MBE).

All samples used in this study were *n*-type Si(100), having a resistivity of ~10 Ω-cm. The samples were cleaned by Ohmic heating to about 1100°C for 10 s; this produced a sharp (2 × 1) 2-domain HEED pattern. The In, Sb, Sn, and Ag overlayers were prepared by evaporation from electron-beam heated crucibles with a typical rate of 1 monolayer (ML) per minute. In this paper, 1 ML of the adsorbate is defined as 6.8×10^{14} atom/cm^2, which is the site density for an unreconstructed Si(100) surface. Owing to the dependence of the various adsorbate-induced reconstructions on the substrate temperature, different sample-preparation temperatures were used for the various adsorbates. The In and Ag were deposited at approximately room temperature. For Sb the substrate temperature was maintained at ~350°C; at this temperature, the Sb coverage saturates at about 1 ML [3]. The room temperature as-deposited Sn surfaces were annealed at 550°C for 2 min; the annealing does not cause any loss due to evaporation or bulk incorporation. All samples were allowed to cool to near room temperature before the photoemission experiments.

3. Results and Discussion

3.1. *Si core-level spectra*

A few typical surface-sensitive Si 2*p* core-level spectra (dots) are shown in Fig. 1 for the clean and Sb-covered Si(100)

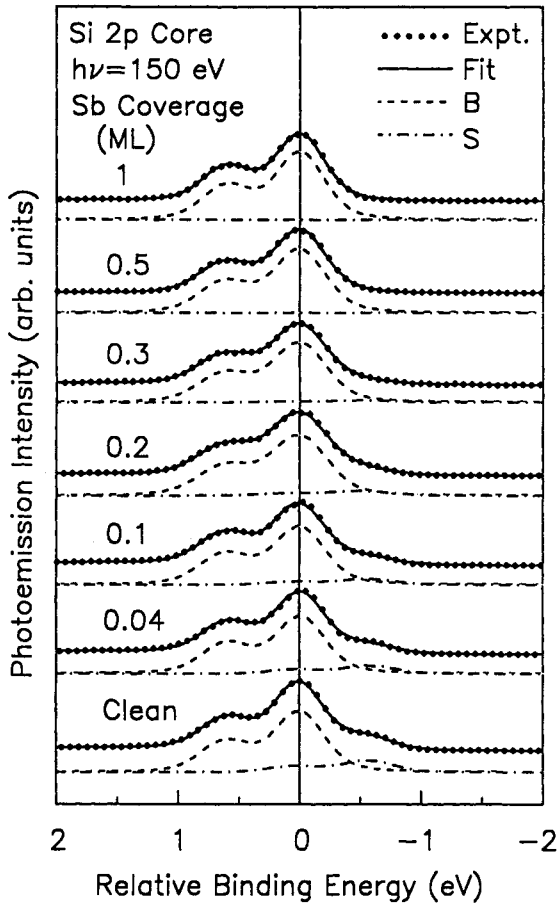

Fig. 1. Si 2*p* core-level spectra (dots) taken with a photon energy of 150 eV for the clean Si(100)-(2 × 1) and Sb-covered Si(100) surfaces. The Sb coverages are indicated. The solid curves are the result of the fit to the data. The decomposition of the spectra into the bulk (B) and surface (S) contributions are shown by the dashed and dashed-dotted curves, respectively. The relative binding energy scale is referred to the Si $2p_{3/2}$ core-level component of the bulk contribution.

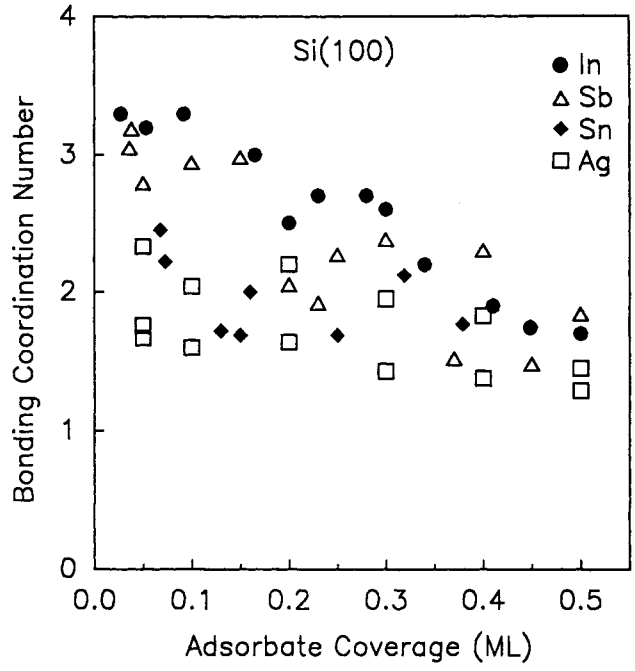

Fig. 2. Adsorbate-to-Si(100) bonding coordination numbers (BCN) as a function of adsorbate coverage. The different symbols correspond to different adsorbates as indicated. For some coverages, more than one data point is shown, corresponding to independent measurements. The data scattering for each adsorbate is due to the limited experimental precision.

surfaces. The spectrum of the clean surface at the bottom of Fig. 1 shows a distinct hump on the lower binding energy side of the main spin–orbit split peaks, which is indicative of a distant surface core-level shift [2–5, 7]. The decomposition of the spectrum into bulk (B) and surface (S) contributions are shown and the nonlinear least-squares fitting procedure has been discussed previously [2–5, 8]. The solid curve running through the data points is the overall fit.

The Si 2*p* core-level spectra for the adsorbate-covered surfaces were analyzed in the same fashion as for the clean case; some of the spectra are shown in Fig. 1. The intensity of the surface component is seen to decrease with increasing Sb coverages, and its positions remains fixed relative to the bulk component. The behavior of the Si 2*p* spectra for In, Sn and Ag deposited on Si(100) is very similar, and for each system the highest coverage which shows a barely detectable S component emission is ~0.5 ML [2–5]. The suppression of the Si surface core-level shift with adsorbate coverage is due to the direct bonding between the adsorbate and the surface Si atoms, which saturates the Si surface dangling bonds and causes the Si surface atoms to become four-fold coordinated as in the bulk [2–5]. Since the binding energy of the reacted Si dimer atoms shifts toward a position which is indistinguishable from the bulk emission, the bonding is essentially covalent in nature. The binding-energy shift caused by adsorption is intimately related to the electronegativity difference between the adsorbate and the substrate [9, 10]. The electrostatic potential at the core is sensitive to the redistribution of valence charge resulting from chemical bonding [9]. Since the electronegativities of In, Sb, Ag, Sn and Si are all similar [11], it is expected that the reacted Si surface atoms should possess a binding energy similar to the bulk value.

By performing an *in situ* comparison of Si(100)-(2 × 1) with Si(111)-(7 × 7), the number of dimer atoms on Si(100)-(2 × 1) which contribute to the S component has previously been measured to be 0.92 ± 0.07 ML [12]. From the intensity reduction of the S component, the average number of Si surface atoms which are modified in the presence of an adsorbate atom, which is the BCN, has been calculated [2–5]. The results are shown in Fig. 2 for the In, Sb, Sn, and Ag covered surfaces as a function of the adsorbate coverages. The uncertainty in the dimer-atom population of the clean surface leads to a systematic error of about 8% in the data; random fluctuations are due to the limited experimental precision. The BCN data in Fig. 2 show basic trends among the various adsorbates. For each adsorbate it is apparent that the BCN gradually decreases as the coverage approaches 0.5 ML. Since ~0.5 ML is the highest coverage which shows a barely detectable S component, the BCN is rigorously defined only up to this point. The In and Sb adsorbates show a similarity in the BCN behavior; the BCN is seen to be about 3 for coverages less than ~0.1 ML and gradually decreases to 2 for coverages approaching 0.5 ML. Likewise, Sn and Ag show similar behaviors, with the BCN remaining close to 2 for lower coverages while exhibiting a slight decrease for higher coverages.

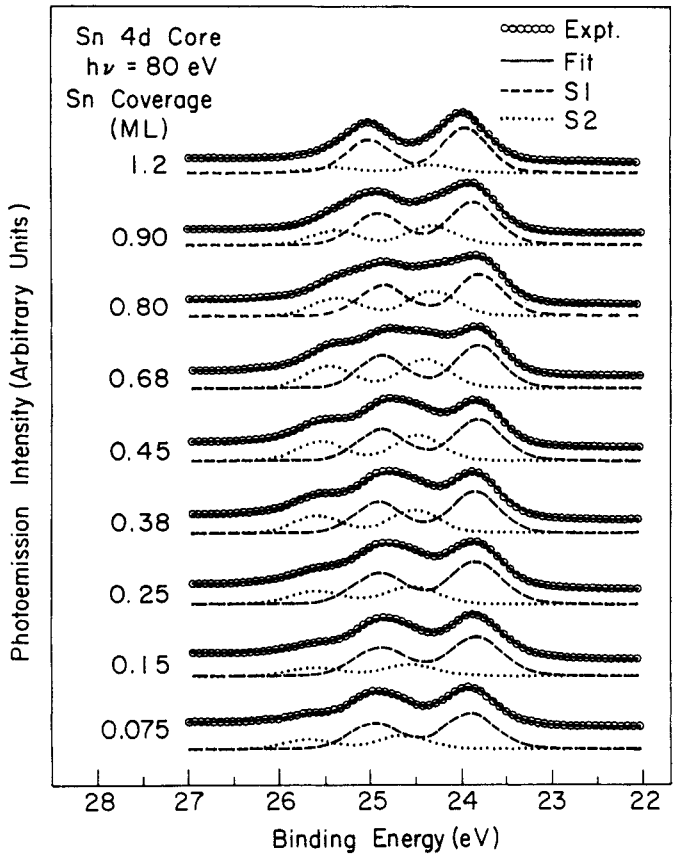

Fig. 3. The Sn 4*d* core-level spectra (circles) taken with a photon energy of 80 eV for various Sn coverages on Si(100). The solid curves are the result of a fit to the data. The decomposition into the S1 and S2 contributions are shown by the dashed and dotted curves, respectively. The binding-energy scale is referred to the Fermi level.

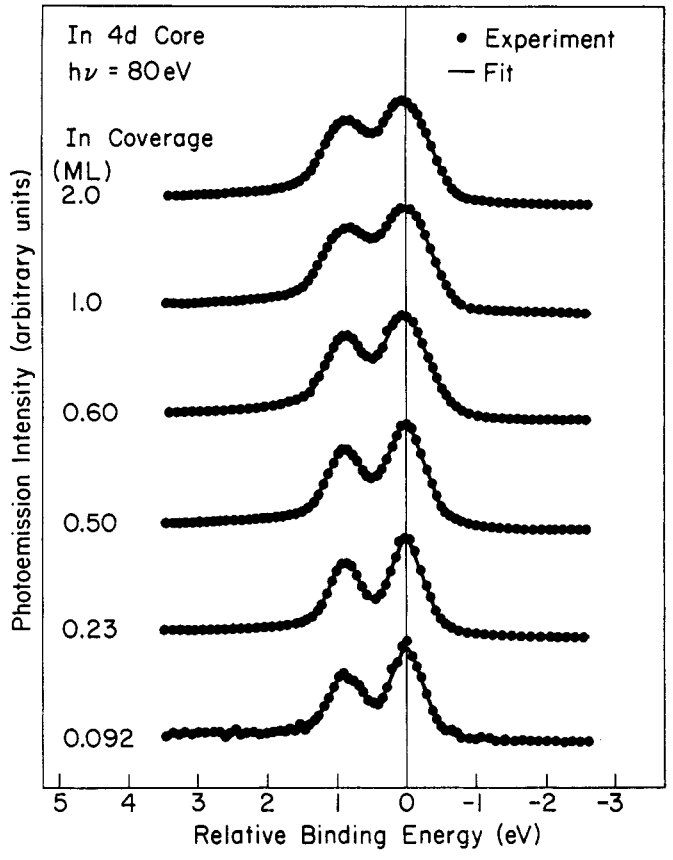

Fig. 4. The In 4*d* core-level spectra (dots) taken with a photon energy of 80 eV for various In coverages on Si(100). The solid curves are the result of a fit to the data. The binding-energy scale is referred to the In $4d_{5/2}$ core level component.

3.2. *Adsorbate core-level spectra*

Information assessing the adsorbate-site bonding can also be acquired from the adsorbate core-level line shapes. Figure 3 shows the Sn 4*d* core-level spectra for various coverages, taken with $h\nu = 80$ eV. The binding energy scale is referred to the Fermi level. The spectra show an additional hump which grows on the higher binding energy side of the main spin–orbit split peak for increasing coverages less than 0.68 ML. For coverages greater than 0.68 ML, this additional hump diminishes in intensity relative to the main peaks. Thus, by this simple visual inspection, it is apparent that there are two distinct components. The least-squares fitting procedure for the Sn 4*d* core-levels is imilar to that described for the Si 2*p* core-level analysis. The lower- and higher-binding energy components are labeled S1 and S2, respectively, in Fig. 3. The S1 binding energy is found to closely parallel the Fermi-level position (as seen in Fig. 3) while the S2 binding energy is approximately a constant relative to the valence-band maximum (VBM) [4]. From the relative intensities of the S1 and S2 components it is possible to determine the population of each Sn-adsorbed site associated with the components for various Sn coverages. The Sn site populations are an important quantity, which, when used with the BCN measurements, will further constrain the number of possible structures.

The In 4*d* core-level spectra are shown in Fig. 4. Unlike the Sn 4*d* core levels, the In 4*d* spectra show no distinct shifts due to the presence of inequivalent sites. The only noticeable change in the line shape for increasing coverages is the increase in the Gaussian width of the peaks. The spectra were fitted by assuming the presence of just one component with variable Gaussian width. The Gaussian width is seen to be approximately constant for coverages less than ~ 0.5 ML, and rapidly increases to a saturation value at 1.0 ML which is about 50% greater than the width measured for the lowest coverages. The absolute energy position of the In 4*d* peaks shifts towards lower binding energies (relative to the Fermi level) for increasing coverages, approximately following the band bending deduced from the Si bulk core and valence levels. The existence of only one In 4*d* component and its relative constancy in width for coverages less than ~ 0.5 ML suggest that essentially all In adatoms occupy chemically equivalent sites (i.e., having similar bonding configurations).

The line shapes of the Sb 4*d* core levels (not shown here) show just one component with a constant width for coverages up to the saturation limit of ~ 1 ML, implying that all Sb adatoms occupy chemically equivalent sites. Ag does not have any intense shallow core level that can be conveniently studied with our instruments; thus, we have no data for Ag/Si(100).

3.3 *Structural model development*

Based on the photoemission and HEED results, the number of allowed structural models for the adsorbate-induced reconstructions becomes considerably reduced and models which correlate well with the data have been proposed. For Sn/Si(100), the BCN is seen to be ~ 2 for low coverages where

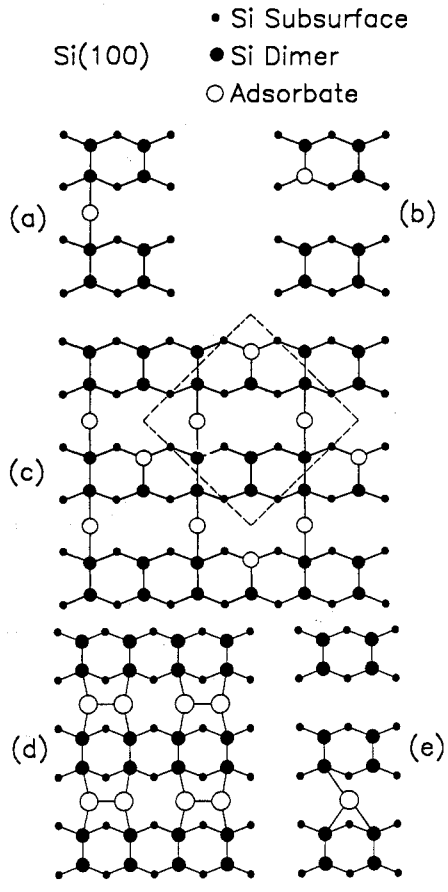

Fig. 5. A picture of structural models for various adsorbate-induced reconstructions on Si(100). This top view of the surface shows the first subsurface Si atomic layer (small dots), Si dimer-atoms (large dots), and the adsorbates (open circles). For Sn adsorbed on Si(100), the portions (a), (d), and (c) are used to illustrate the S1 site, S2 site, and $c(4 \times 4)$ reconstruction, respectively. For In adsorbed on Si(100), the portions (d) and (e) are used to illustrate the fully developed In (2×2) dimer structure and a lone In-adsorbed site, respectively. Portion (a) is also used to indicate a lone Ag site position for Ag/Si(100).

the Sn 4*d* spectra of Fig. 3 show a predominance of S1 sites. Figure 5(a) shows the adsorption position for an S1 site which is located in a bridge site midway between two dimers. Such two-fold bonding corresponds to a bicovalent s^2p^2 electronic configuration, with an unshared *s*-electron pair and two *p*-bonding orbitals. In Fig. 5(b) a Sn replacement site describing the S2 sites is shown for which a Sn adatom replaces the tetrahedral configuration of a Si dimer atom. This replacement site should sense the full band bending of the Si host lattice, and indeed, the S2 site binding energies are found to correlate with the VBM position [4]. This is further supported by the BCN measurements which show that the Sn-to-Si BCN decreases below 2 for higher coverages which have a relatively greater S2 population. A Sn-induced *c* (4×4) reconstruction is observed at 3/8-ML coverage from HEED [4, 13], and a structural model which illustrates this is shown in Fig. 5(c). A $c(4 \times 4)$ unit cell is outlined by the dashed lines. The model exhibits a basis of three Sn adatoms, with two S1-type atoms and one S2-type atom. The ratio of sites S2 and S1 is 1 : 2, consistent with the results of Fig. 3. The predicted BCN for this structure is 5/3, and agrees with the BCN results of Fig. 2. This structure, however, is not unique since by changing the S2-atom locations within the unit cell, one can generate equally consistent structural models.

For In/Si(100), HEED measurements show a (2×2) pattern which appears at low coverages and is fully developed at ~ 0.5 ML, followed by another In-introduced (2×1) pattern after 0.5 ML [1, 14]. The results shown in Fig. 2 indicate that the BCN is 3 for low coverages and gradually approaches ~ 2 for coverages approaching 0.5 ML. A simple structure at 1/2-ML coverage is illustrated in Fig. 5(d). The In adatoms form dimers with the dimer bond rotated 90° with respect to the Si dimer bond and this results in a (2×2) periodicity for a coverage of 1/2 ML. The valency of In would indicate an approximate sp^2 trigonal bonding configuration as shown. An isolated In adsorption position is shown in Fig. 5(e); In-dimerization is expected to be reduced at extremely low coverages where the In is mainly dispersed over the surface in the form of a 2-D gas [1, 4]. The predicted BCN is 3, in agreememt with experiment. For coverages greater than 0.5 ML, the In is expected to fill in the saturated In (2×2) structure resulting in new bonding configurations; the rapid increase of the Gaussian width of the In 4*d* core level spectra of Fig. 4 for coverages in excess of 0.5 ML confirms this.

For Ag/Si(100) the results of Fig. 2 indicate that the BCN is ~ 2 for low coverages. Therefore, we propose the model shown in Fig. 5(a) for this system. Ag molecules are commonly found to exist in bicovalent and linear bonding geometries (e.g., such as the covalent $Ag[NH_3]_2^+$ and $Ag[CN]_2^-$ molecules), and the site in Fig. 5(a) is characterized by this kind of bonding. The Ag growth on Si(100) is known to involve the formation of Ag(111) metallic islands [15, 16], and from the Ag 4*d* valence-band line shapes, it has been found that a significant Ag aggregation occurs for coverages less than 1 ML. Thus, the decrease in the BCN below the initial value of 2 for low coverage is consistent with the formation of Ag islands, leading to an increased Ag-Ag and a reduced Ag–Si interaction.

The BCN results for Sb are similar to those for In. Since both Sb and In are primarily valence-3 materials, the bonding is expected to be similar. Our recent STM results indicate clearly the bonding of Sb to the Si dangling bonds; the Si dimer structure remains intact under an Sb adlayer which shows considerable disorder [3]. The disorder is likely due in part to the large size match between Sb and Si.

Acknowledgements

This material is based upon work supported by the Department of Energy, Division of Materials Sciences, under Contract No. DE-AC02-76ER01198. Some of the personnel and equipment support was also derived from grants from the National Science Foundation (Grants No. DMR-8352083 and No. DMR-8614234). We acknowledge the use of central facilities of the Materials Research Laboratory of the University of Illinois, which was supported by the Department of Energy, Division of Materials Sciences, under Contract No.DE-AC02-76ER01198, and the National Science Foundation under Contract No. DMR-8316981.

References

1. Hamers, R. J., Tromp, R. M. and Demuth, J. E., Phys. Rev. **B34**, 5343 (1986).
2. Rich, D. H., Samsavar, A., Miller, T., Lin, H. F., Chiang, T.-C., Sungdren, J. -E. and Greene, J. E., Phys. Rev. Lett. **58**, 579 (1987);

Rich, D. H., Samsavar, A., Miller, T., Lin, H. F. and Chiang, T.-C., Mater. Res. Soc. Symp.Proc. **94**, 219 (1987).
3. Rich, D. H., Leibsle, F. M., Samsavar, A., Hirschorn, E. S., Miller, T. and Chiang. T. -C., Phys. Rev. **B39**, 12758 (1989); Rich, D. H., Miller, T., Franklin, G. E. and Chiang, T. -C., Phys. Rev. **B39**, 1438 (1989).
4. Rich, D. H., Miller, T., Samsavar, A., Lin, H. F. and Chiang, T. -C., Phys. Rev. **B37**, 10221 (1988).
5. Samsavar, A., Miller, T. and Chiang, T. -C., Phys. Rev. **B38**, 9889 (1988).
6. Hulbert, S. L., Stott, J. P., Brown, F. C. and Lien, N., Nucl. Instrum. Methods **208**, 43 (1983).
7. Himpsel, F. J., Heimann, P., Chiang, T. -C. and Eastman, D. E., Phys. Rev. Lett. **45**, 1112 (1980).
8. Miller, T., Hsieh, T. C. and Chiang, T. -C., Phys. Rev. **B33**, 6983 (1986).
9. Chiang, T. -C., CRC Crit. Rev. Solid State Mater. Sci. **14**, 269 (1988); Mat. Res. Soc. Symp. Proc. **143**, 55 (1989).
10. Joyce, J. J., Grioni, M., del Giudice, M., Ruckman, M. W., Boscherini, F. and Weaver, J. H., J. Vac. Sci. Techol. **A5**, 2019 (1987).
11. Sanderson, R. T., Chemical Bonds and Bond Energy. Academic, New York (1971).
12. Rich, D. H., Miller, T. and Chiang, T. -C., Phys. Rev. **B37**, 3124 (1988).
13. Ueda, K. and Kinoshita, K., Surf. Sci. **145**, 261 (1984).
14. Knall, J., Sungdren, J. -E., Hansson, G. V. and Greene, J. E., Surf. Sci. **165**, 512 (1986).
15. Hanbucken, M., Futamoto, M. and Venables, J. A., Surf. Sci. **147**, 433 (1984).
16. Samsavar, A. and Chiang, T. -C, Unpublished STM results.